Annually-resolved lake record of extreme hydro-meteorological events since AD 1347 in NE Iberian Peninsula

J.P.Corella[1], G. Benito[1], X.Rodriguez-Lloveras[1], A. Brauer[2], B.L. Valero-Garcés[3]*

[1]Museo Nacional de Ciencias Naturales, (MNCN-CSIC, Serrano 115bis, 28006 Madrid, Spain. E-mail address: pablo.corella@mncn.csic.es, benito@mncn.csic.es, xavi.rodriguez@mncn.csic.es

[2]Deutsches GeoForschungsZentrum Potsdam, Sektion 5.2 Klimadynamik und Landschaftsentwicklung, D-14473 Potsdam, Germany. E-mail address: brau@gfz-potsdam.de

[3]Instituto Pirenaico de Ecología (IPE-CSIC), Avda Montañana 1005, 50059 Zaragoza, Spain. E-mail address: blas@ipe.csic.es

(*) Corresponding author:

E-mail: pablo.corella@mncn.csic.es

Postal address: Museo Nacional de Ciencias Naturales (CSIC), Serrano 115bis 28006 Madrid (Spain)

Telephone: +34 917452500 ext. 980603

Fax: +34 915640800

ABSTRACT

We present an annual reconstruction of extreme rainfall events interpreted from detrital layers and turbidites interbedded within a varved sediment record since the 14th century in Montcortés Lake (NE Spain, 1027 m a.s.l.). Clastic microfacies intercalated within the biochemical calcite varves were characterized and their depositional dynamics interpreted using high-resolution geochemical and sedimentological analyses. Annual number of detrital layers was compared against instrumental records of extreme daily rainfalls providing minimum rainfall thresholds and return periods associated to the identified types of clastic microfacies. Non-continuous detrital layers were deposited during rainfall events higher than 80 mm (> 2-year return period) while graded detrital layers and turbidites were associated with higher magnitude rainfall events (> 90mm and >4-year return period). The frequency distribution of extreme hydro-meteorological events is not stationary and its pattern coincides with historical floods from the nearby Segre River. High frequency of heavy rainfalls occurred during the periods AD 1347-1400 and AD 1844-1894. A lower frequency of heavy rainfall was found during the periods AD 1441-1508, 1547-1592, 1656-1712, 1765-1822 and 1917-2012. The 20th century stands out as the longest interval within the studied period of very low number of extreme rainfall events. Variability in extreme rainfall events prior to the 20th century is in phase with solar activity, suggesting a mechanistic link in mid-latitude atmospheric circulation patterns that ceased during the 20th century.

Keywords: Extreme rainfall, Palaeofloods, Microfacies, Lacustrine varves, Solar activity, Climate Change

1- INTRODUCTION

Floods and storms are the most devastating natural disasters in terms of casualties and economic losses due to infrastructures damage (Kundzewicz et al., 2014). In the context of current global warming, there is a high uncertainty on the observed trends and projected changes in heavy rainfall and floods at a global scale (Seneviratne et al., 2012). For example, in Europe, there are regions recording a statistically significant increase in heavy precipitation events during the last decades, e.g. central Europe (Zolina et al., 2008; Kyselý, 2009) and others show with significant decreases in winter precipitation extremes - e.g. Mediterranean coastal sites; (Toreti et al., 2010) -, and even within these regions there are strong sub-regional or local variations. Uncertainties are overall larger in southern Europe and the Mediterranean, where confidence in secular trends is low (Hartmann, , 2013)

Understanding the spatial and temporal scale at which changes on hydrological extremes occur in response to climatic variability is essential to anticipate climate change impacts and to implement adaptation and mitigation measures in relation to natural hazards. Another important issue in climate change science is the detection and attribution of human influence on the heavy precipitation trends and, therefore, in the hydrological cycle (Min et al., 2011). Detection of temporal changes on extreme events requires long-term records to overcome the problems derived from their high inter-annual and inter-decadal rainfall variability, particularly in Mediterranean climates (Machado et al., 2011). Moreover, attribution entails a profound knowledge of the natural variability of the water cycle at fine enough resolution, identifying all potential drivers of hydrological change (Hattermann et al., 2012).

Paleohydrological studies play here an important role as they enable us to investigate the dynamics of extreme events under natural climate variability beyond the instrumental period, as well as to evaluate the main forcings controlling the hydrological cycle. Numerous studies have been carried out during the last decades to quantify the magnitude and recurrence periods of extreme rainfall events and subsequent flood events, e.g. (Knox, 1985; Noren et al., 2002; Czymzik et al., 2013). Among natural archives, fluvial and lake records are most adequate to carry out reconstructions of hydrological extremes. Palaeoflood studies in bedrock rivers are typically based on stratigraphic descriptions of slack-water flood sediments deposited during high flood stage at high elevation zones from which robust discharge estimates can be obtained based on hydraulic modeling (Baker, 2008; Benito and O´Connor, 2013). In these fluvial environments, only the largest floods exceeding the elevation of previous flood deposition threshold are recorded (Thorndycraft et al., 2008).

Lake sediments have proven to be a valuable archive of recurrence rates and intensities of past floods as they constitute the natural sink for sediments transported by rainfall-induced run-off (Czymzik et al., 2013; Gilli et al., 2013). The advantage of lake sequences for palaeoflood reconstructions is their high preservation potential and their capability to record a wider range of runoff events from medium to high magnitude flows. During the last decade, numerous records in European lakes have improved our knowledge of the hydrological fluctuations during the Late Holocene (Gilli et al., 2003; Moreno et al., 2008; Bussmann and Anselmetti, 2010; Debret et al., 2010; Giguet-Covex et al., 2012; Swierczynski et al., 2012; Wilhelm et al., 2012; Czymzik et al., 2013; Swierczynski et al., 2013; Vanniere et al., 2013). Among them, flood deposits intercalated in varve sequences provide the most accurate chronologies, with annual to seasonal resolution (Czymzik et al., 2010; Swierczynski et al., 2012; Czymzik et al., 2013; Swierczynski et al., 2013; Vanniere et al., 2013). Recent studies in European varve sequences have linked Late Holocene variations in solar irradiation with North

Atlantic atmospheric circulation shifts, e.g. (Martin-Puertas et al., 2012), and with frequency of heavy summer rainfall leading to higher flooding frequency during solar minima in the Alps (Czymzik et al., 2013; Wirth et al., 2013a). So far, varve sediment-based flood reconstructions are restricted to the alpine region and not available, for example, for the Mediterranean area. Lake Montcortès is an exceptional site to reconstruct past flood events as the sedimentary record preserves different types of flood-related detrital layers with annual to seasonal resolution over the last 3500 years (Corella et al., 2011). Sedimentological analyses in two well-preserved gravity cores have been performed to achieve the following objectives: i) to interpret the depositional dynamics of the different detrital micro-facies; ii) to evaluate the sensitivity of the record to rainfall variability by comparison with instrumental time series; iii) to carry out an annually-resolved palaeohydrological reconstruction of extreme rainfall since the 14th century and; iv) to compare the lake record with other sources of information such as historical floods reported from documentary archives in the nearby rivers, leading to an improved and comprehensive view on the hydrological variability in the NE Iberian Peninsula during the last millennia.

2- STUDY SITE

Lake Montcortès is located in the southern Central Pyrenees, in Catalonia region (NE Spain) (42º19.50'N, 0º59.41'E, 1027 m a.s.l.). The watershed (1.39 km^2 surface area) is emplaced between Les Nogueres and the South Pyrenean structural units, composed by Mesozoic and Tertiary sedimentary units tectonically thrusted southwards. The watershed lies on Oligocene conglomerates (36% of the total catchment area), and siliciclastic, carbonate and evaporitic Mesozoic rocks (Keuper and Muschelkalk facies, 24% of the total area), with some hypovolcanic ophite bodies are also present in the southern areas of the watershed (8%); Quaternary sediments outcrop around the lakeshore (7%) (Fig. 1). The origin of the lake is attributed to interstratal dissolution and collapse of Keuper evaporites (Corella et al., 2012). The land use in the watershed mainly consist on cereal crops, meadows and pastures in the lowlands (60% of the total area) and deciduous and conifer forests in elevated areas (30%) (Fig. 1). Hygrophytic communities colonize the lakeshore. Lake Montcortès basin is almost circular, with a surface area of 0.14 km^2 (10% of the catchment area, Fig. 1) and a maximum depth of 30 m, and with very steep margins. There are two ephemeral streams that drain the southern area of the watershed providing water and sediments to the lake mainly during extreme rainfall events (Fig. 1). The maximum lake level is controlled by an outlet stream in the northern shore. No quantitative water balance is available for the lake, but groundwater is a significant input. The lake´s water column has permanent annual stratification that allows the preservations of biogenic varves (Corella et al., 2012). The coldest and warmest months have average temperatures of 1.9ºC (January) and 20.3ºC (July). Mean annual rainfall in the area is 860 mm. Heavy rainfall (>100mm) in the region occurs mainly in autumn (50%) and winter (22.1%) (Martin-Vide et al., 2008). Autumn and spring heavy rainfall events are associated with mesoscale convective systems fed by Mediterranean moisture and enhanced by the orography of the eastern pre-Pyrenean Mountains (Llasat and Puigcerver, 1994). Rainfall it is also influenced, although on a lesser extent, by frontal Atlantic systems generating persistent rainfall during the autumn and winter months. Indeed, in this area the highest magnitude precipitation events are related to negative phases of North Atlantic Oscillation (NAO) (Vicente-Serrano et al., 2009).

3- MATERIALS AND METHODS

3.1 Sediment coring

Previous studies (Corella et al., 2011) have shown the occurrence of mass wasting deposits and gravitational slides in the distal areas of Montcortés Lake that could compromise the recovery of undisturbed sediment sequences at some locations. Therefore, several seismic profiles were acquired with a high-resolution, single channel Edge-Tech sub-bottom profiling systems to determine optimal core location for undisturbed sediments. Two UWITEC gravity cores (MON12-3A-1G, 78 cm length, and MON12-2A-1G, 106 cm length) were retrieved using the coring equipment from the Pyrenean Institute of Ecology (IPE-CSIC) at the deepest area (~ 30 m depth) of the lake, where the seismic profiles displayed parallel reflections indicating undisturbed sediments. Distance between coring sites is 30m. Hammering was avoided during coring operations at site MON12-3A-1G to minimize sediment disturbance, but it was necessary to retrieve the longer core MON12-2A-1G. A composite sedimentary sequence 104-cm long was obtained by detailed varve correlation between both cores. The sediment cores were carefully transported to the lakeshore and stored there for 5 days to favor sediment consolidation before transport to the IPE cold-room.

3.2 Laboratory analyses

The sediment cores were split lengthwise. X-ray fluorescence element scanning was analyzed at the University of Barcelona using an AVAATECH XRF core scanner (2000 A, 10-30kV and 20-50 s measuring time) every 0.2 mm. The resulting intensities for major elements - potassium (K), calcium (Ca) and zirconium (Zr) – are giving as counts per second (cps), providing semiquantitative information of the elemental composition of the sediments. Core images were obtained by using the high resolution AVAATECH core scanner coupled camera. The upper 43 cm of the sedimentary sequence was analyzed every 1 cm for Total (TC) and inorganic (TIC) carbon with a LECO 144DR elemental analyser. Total organic carbon (TOC) was calculated by subtracting TIC from TC. Microfacies analyses were carried out by detailed inspection of large-scale thin sections (120mm X 35 mm) prepared after sampling in aluminum trays, freeze-drying and impregnation in Epoxy resin following the methodology described by (Brauer and Casanova, 2001). Sediment composition and layer thickness were described and measured using a *Nikon Eclipse E600* microscope from the MNCN-CSIC microscope lab. A *Nikon AZ100M* X-ray fluorescence microscope from the GFZ (Potsdam) was used to identify and photograph organic sediment components.

3.3 Dating

Calcite varve counting was performed by double counting by one investigator in 14 overlapping thin sections (2 cm overlap). Detailed correlation with a previously published chronology (Corella et al., 2012) was carried out to assess the error from the previous age model. The former chronology was developed on a long core obtained with a Kullenberg device (MON04-3A-1K). Core correlation between both cores was carried out by utilizing marker layers – mostly detrital layers – unequivocally identified in both sediment cores. An independent radiometric age model was obtained in a parallel core MON08-3A-1U, where excess ^{210}Pb activity was analyzed using an Ortec alpha spectroscopy system (St. Croix Watershed Research Station, Minnesota) to determine the age and sediment accumulation rates for the past 100-150 years. Thirteen measurements with variable resolution were carried out in the first 47 cm of sediment. Unsupported ^{210}Pb was calculated by subtracting supported activity from the total activity measured at each level. The age model was determined by using the constant rate of supply (CRS) proposed by Appleby (2001).

3.4 Historical floods

The historical dataset of floods in the Segre River and other eastern Pyrenean rivers were obtained from the Historical Floods National Catalogue (Comisión Técnica de Inundaciones, 1985a, b) and complemented with other previous compilations such as those of Rico Sinobas (1850), Bentabol (1900), Masachs (1948, 1950), Fontana-Tarrats (1976), López-Bustos (1981), Font (1988), Benito et al. (1996), Llasat et al. (2005), Barriendos and Rodrigo (2006). Further bibliographical sources consulted include scientific and technical reports, local history works and newspapers. Most of the indirect information has been checked by cross-referencing between different sites.

3.5 The instrumental series

The daily maximum precipitation for the period 1917-1994 was obtained from Cabdella meteorological station about 15 km north of the lake (Fig. 1) at 1200 m.a.s.l.-. This meteorological station was selected for comparison with Lake Montcortès record because it is the nearest station with the longest, most reliable and complete daily precipitation records. Only three months for the entire 1917-1994 period are missing (July 1920, November 1937 and February 1938). The square-root exponential type distribution of the maximum (SQRT-ET^{max}) function (Etoh et al., 1987) combined with the maximum likelihood method was applied to estimate extreme events recurrence rates.

4- RESULTS

4.1- Turbidites and Detrital Microfacies in Lake Montcortès

Microfacies

The Lake Montcortès sequence consists of biogenic varves composed of (i) endogenic calcite that precipitates in spring and summer. Biologically induced calcite precipitation in Lake Montcortès occur during algal blooms, mainly diatoms in Lake Montcortès

(Scussolini et al., 2011). CO2 is consumed by increase bioproductibity in epilimnetic waters until calcite solubility threshold is reached and calcite precipitates (Corella et al., 2012), (ii) Organic detritus deposited throughout the year (Corella et al., 2012) (Fig. 2A). Additionally, detrital layers are commonly intercalated within the varve succession and also some turbidite layers punctuate the record. This study focuses on these detrital event layers of the undisturbed uppermost 104 cm sequence that correspond to the top three sedimentological units previously defined by Corella et al. (2011).

Three main types of detrital microfacies have been distinguished in the varves (Fig. 2): i) non-continuous detrital layers; ii) continuous detrital layers; iii) matrix-supported layers. In addition, two types of turbidite layers have been identified.

Non-continuous detrital layers (N-C DL, Fig 2B) consist of small clay-silt homogeneous patches of allochthonous siliciclastic material with poor spatial continuity. 56 N-C DL have been recognized in the studied interval, and in four cases, two layers occurred within one year. Layer thickness ranges from 0.08 to 1mm.

Continuous detrital layers (DL, Fig. 2C) are characterized by a normal grading from coarse-medium silt to clay with no micro-erosion features in the lower boundary. They show a lateral spatial continuity in the studied sediment cores. In total, 152 DL have been identified in 97 varves with layer thickness ranging from 0.2 mm to 1 cm. Up to four DL can occur within one year. Both N-C DL and DL have a mineralogical composition dominated by clay minerals, quartz and feldspar, showing almost negligible organic matter contents.

Matrix-supported layers (ML) are very scarce in the sequence with only 14 cases (Fig. 2D). ML are homogeneous and consist of coarse to fine silt particles of endogenic calcite, reworked littoral carbonates with abundant benthic diatoms and littoral fauna. Layer thickness ranges from 0.4 to 3.6 mm with average thickness of 1.3 mm.

In addition to these three types of detrital layers, cm-thick brownish turbidites, intercalate in the sequence, particularly in sedimentological unit II (Fig. 3). They are recognized by a coarse basal sub-layer (Figs 2E and F), a fining upward texture, and frequent evidences of scouring and micro-erosion of the underlying layers. Two different types of turbidites can be distinguished by their geochemical, mineralogical and textural characteristics (Fig. 2).

Flood turbidites (F-T) (Fig 2E) display a thin sub-layer of coarser particles (average grain-size 0.2 mm) and a well-developed fining upward grain-size distribution. F-Ts are mainly composed of quartz and feldspar at the base of the layers, capped with a finer clay-rich layer. Littoral reworked carbonates and terrestrial organic matter are minor components. A few F-T layers show a subtle grading inversion (Fig. 2E). Layer thickness ranges from 0.8 mm to 2.5 cm average thickness of 0.48 mm. 46 F-Ts have been identified in the sequence.

Mass-movement turbidites (M-T) (Fig. 2F) show a rather thick and homogeneous coarser basal sub-layer (average grain-size 0.4 mm) followed by finer sediments with a fining upward texture. They occur 14 times in the studied interval. Multiple coarse fraction pulses are frequent in this type. Reworked littoral carbonate is the most abundant component, followed by siliciclastic material, and littoral fauna and benthic diatoms (Fig. 2). These deposits are the thickest observed in the sedimentary sequence ranging from 1.2 mm to 3.6 cm with average thickness of 1cm. TOC values are low in both types (1-2%) (Fig. 3) although microscopic observations reveal organic matter remains in thick M-T turbidites as shown in XRF photographs (Fig. 2F).

Geochemistry

The µ- X- ray fluorescence downcore profiles of Zr, K and Ca show a coherent pattern with microfacies variability (Fig. 2 and 3). Calcium follows the same trends than the

TIC profile and it mainly reflects the endogenic calcite content in the biogenic varves, better developed in unit I and III (Fig. 3). On a lesser extent it is also related to the presence of reworked littoral carbonate, which is particularly frequent at the base of M-T turbidites (Fig. 2F).

The Ca/K ratio is an indicator of carbonate content *vs*. siliciclastic input to the lake. It also points out the presence of biogenic varves without detrital layers *vs* detrital microfacies occurrence, although detrital carbonate is also present in detrital layers and should be considered. This ratio follows the TOC curve, with higher carbonate and organic matter in intervals with more abundant biogenic varves and less detrital layers (unit I up to 7% of TOC, Fig. 3).

Zr and K have been selected as proxies for grain-size distribution. Zr, which is generally related to resistant minerals, increase in coarse grained sediments (coarse silt) while K abundance increase in fine structures (clay-minerals) (Cuven et al., 2010). The relation between grain-size distribution and the relative abundance of these elements can be seen in Figs 2 and 3. Therefore, these elements enable identification of fining upward structures (Fig. 3, unit II). Both elements show opposite patterns within turbidites and allow recognition of distinct pulses within a single layer (Fig. 2). Moreover, both Zr and K can be used for microfacies identification, as Zr show peaks in the coarse basal sub-layer of turbidites while K is dominant in clay-rich microfacies N-C DL and DL.

4.2- Chronology

An independent absolute varve chronology was obtained from the composite sedimentary sequence (sediment cores MON12-3A y MON12-2A) from 2012 back to 1347 AD. The chronology for AD 2012 - 1584 was achieved in core MON12-3A due to the best preservation of the varves in this core. Varve counting for the time interval AD

1584 - 1347 was performed in sediment core MON12-2A. Core correlation was carried out by detailed inspections of thin sections in both sediment cores. Short intervals with poor varve preservation constitute only 1% of the studied sequence. These intervals were interpolated by using the mean varve thickness of the upper and lower centimeters of these intervals. Another possible source of error in the current chronology is the occasional micro-erosion or varves below a turbidite deposit, as underflow events may lead to microscopic scouring of the sediments underneath. Previous studies, however, have shown that micro-erosion by graded layers likely causes only few missing varves (Mangili et al., 2005). Nevertheless, the possibility of missing varves is restricted particularly to unit 2 (AD 1844 - 1902) where turbidite layers with erosive contact are most frequent (Fig. 4). Therefore, we consider our varve chronology for Unit 2 (1844 - 1902 AD) based on the identification of calcite layers in the sedimentary record as a minimum chronology.

This new varve chronology presented here improves the chronology established on previous cores (Corella et al., 2012). 36 varves were wrongly added in the old age model in disturbed intervals during the period 1844 -1347. Detailed core to core correlation demonstrates that no missing varves occurred in these disturbed sections. Therefore, the current chronology differs a 7% (less varves) in relation to the previous varve counting. The intervals where varves need to be interpolated are considerably reduced in the new sediment core (only 1% interpolation compared to 5% in the previous chronology). Especially the upper sediments are considerably better preserved in the new cores than in the Kullenberg core MON04-3A-1K (Corella et al., 2012) due to the coring techniques (UWITEC gravity coring without hammering), and careful handling and storing of the cores for a few days at the lakeshore before transport. Our results confirm the advantage of parallel cores to bridge disturbed intervals in one core by better preserved sections in the other undisturbed cores (Brauer et al., 2008; Ojala et al., 2012).

To identify undetected systematic errors in the current varve-based age-depth model, two independent dating methods were used. Varve counts are supported by one AMS ^{14}C date (Corella et al., 2011) and by excess ^{210}Pb dating obtained in the upper 15 cm of a parallel core (MON08-1B, Fig. 1 and 4). The excess ^{210}Pb profile displays a decrease in depth ranging from 6.36 pCi/g near-surface to 1.39-1.05 pCi/g at 10-11 cm below the surface. The estimated supported ^{210}Pb (^{214}Pb) (9 samples) is of 0.84± 0.02 pCi/g. The lower values of excess ^{210}Pb at 12-15 cm (0.73-0.29 pCi/g) correspond to thick turbidite layers from unit 2 (Fig. 4) that is an instantaneous deposit and has been avoided for constraining the ^{210}Pb age model, e.g. (Arnaud et al., 2002). Constant rate of supply (CRS) modeling of the ^{210}Pb activities gives a date of AD 1905 at 11cm (boundary between sedimentological units 1 and 2, Fig. 4), which is coherent with the varve chronology for this boundary layer dated at AD 1903. The agreement between these independent chronologies supports the robustness of the revised varve chronology for the last 100 yrs displaying a similar sedimentation rate of 0.1cm/yr during the 20th century.

4.3- Detrital microfacies as a proxy for maximum daily precipitation

The comparison between the detrital microfacies in Lake Montcortès with the instrumental daily rainfall record from 1917 to 1994 shows a clear relation between extreme precipitation events and detrital layers deposition (Table 1, Fig 5). Eleven detrital layers have been identified in this period. Nine of them match exactly with measured extreme rainfall events. In the case of the other two flood layers (AD 1973 and 1951) we observed a difference of 1 year between the layer deposition and the extreme rainfall. This difference might be related to the annual biochemical cycle of calcite precipitation in the lake. Calcite layers form in late spring to summer and the floods occurred in March and June at 1952 and 1974 respectively. Therefore, delayed calcite precipitation in summer due to longer winters and colder temperatures would explain this chronological mismatch.

Minimum rainfall thresholds - referred as annual maximum daily precipitation (MDP) – have been estimated based on comparison between the instrumental record and the clastic microfacies occurrence (Fig. 5). Therefore, N.C DL deposition has always occurred since AD 1917 when rainfall events exceeded 80 mm MDP, F-T layers occurred during rainfall events exceeding 91.5 mm MDP and DL for rainfall events exceeding 101 mm MDP. Recurrence rate estimations from the instrumental time-series show return periods of 2, 3, 5 and 8 yrs for rainfalls above 80, 90, 100 and 110 mm MDP, respectively (Fig. 5). Three large magnitude precipitation events between 1987 and 1993 are not associated to clastic layers in the sedimentary record (Fig. 5), which might be due to sediment disturbance in the upper 2 cm of sediment. An alternative explanation is that those precipitation events responded to local thunderstorms that did not affect the Montcortès watershed, as such heavy rainfall was not recorded in other meteorological stations in the region. Nevertheless, a large increase of K and Zr during that interval suggests an input of allochthonous –both coarse and fine- material to the lake during those years.

A total of seven out of ten precipitation events > 100 mm (5-year return period) between 1917 and 1987 are reflected in the sedimentary record (three DL, two FT and two N.C. DL, Fig. 5). Four events exceeded 109 mm (8-year return period) during that period and all of them are preserved in the sediments. The two maximum rainfalls of the instrumental record (1982, 252 mm, and 1937, 160 mm) coincide with historical floods in the Segre River and are represented in Montcortès as one FT and one DL. Four flood layers (2 FT and 2 N.C. DL) out of 16 rainfall events between 80 and 100 mm (2-5-year return periods) have been detected, showing a lower sensitivity of the depositional dynamics to record precipitation events of that intensity, as only 25% of are recorded as detrital event layers in Lake Montcortès.

4.4 Detrital layer frequency since AD 1374 to Present

Within the studied interval since AD 1347 we distinguish 13 decadal-scale periods that differ in frequency and thickness of detrital layers (Table 2) and can be classified in periods with high, low and intermediate detrital layer deposition. The highest frequency of detrital layers (average of 1.25 events/ year) occurred during the periods AD 1347-1400 and AD 1844-1894 comprising a total of 103 layers with an average thickness of 1.55 mm. and the highest frequency of DL and FT.

In contrast, the periods AD 1441-1508, 1547-1592, 1656-1712, 1765-1822, 1917-2012 are characterized by low frequencies and thickness of detrital layers (mean frequency of 0.23 events/year, mean thickness of 0.93 mm). Detrital layer occurrence in the intervals AD 1401-1440, 1509-1546, 1593-1655, 1713-1764, 1823-1843, 1895-1916 is intermediate with a mean detrital layer thickness of 0.4 mm and an average of 0.4 events per year.

5- DISCUSSION

5.1- Depositional models for detrital microfacies

The textural and geochemical signatures indicate different modes of deposition of detrital layers in Lake Montcortès:

The graded structure and the lack of micro-erosion features suggest low-density currents as the depositional process for detrital layers (DL). The sediment plumes are not sufficiently dense to pervade the thermocline formed by the permanent water stratification of the meromictic lake so that suspended matter is distributed within the lake basin through overflows and interflows. Differential settling of suspended particles according to their grain-size leads to the observed fining upward textures. The same process can be envisaged for deposition of non-continuous detrital layers (N.C. DL). Finer grain sizes and reduced thickness of these layers may suggest less energetic flows in the catchment. Fine sediments may either flocculate with a fast deposition in the lake bottom or remain days to weeks in the water column before settling down. During that time, internal lake currents might lead to an uneven spatial distribution of detrital material on the lake bottom explaining the patched morphology and the lack of grading of these deposits.

The depositional mechanisms of matrix-supported layers (ML) are not straight-forward and include several processes in the talus (mass wasting) and the watershed (floods) (Mangili et al., 2005; Czymzik et al., 2010; Swierczynski et al., 2012). In Montcortès, the abundant reworked littoral material suggest local slumping and talus reworking driven by internal lake processes including wave activity and mass-wasting induced by sediment loading.

Turbidite deposits are the result of density currents that occur when sediment laden inflows are denser than the ambient lake water, penetrating through the lake stratification as underflows (hyperpycnal flow) (Mulder and Syvitski, 1995; Sturm and Matter, 1978; Corella et al., 2013a). Sedimentological indication for underflows is the observed erosive boundaries and the re-entrainment of reworked littoral material. Turbidite flows could be triggered by major floods and/or mass-movements from slopes instabilities e.g. (Sturm et al., 1995; Mulder et al., 2001; Karlin et al., 2004; Girardclos et al., 2007; Osleger et al., 2009). However, discerning both triggers in each individual turbidite layer is needed to avoid over- or underestimations in the frequency of either floods and/or mass-movements. In Lake Montcortès, sedimentological and compositional signatures of turbidites enable us to distinguish between flood and mass-movement deposits.

Mass- movement Turbidites (M-T) are characterized by thick and homogeneous basal sub-layers, multiple coarse grain-size pulses occurring during individual events and generally thicker deposits, all common features of mass-movement- induced gravity flows (Gorsline et al., 2000; Mulder et al., 2001; Mulder et al., 2003; Wirth et al., 2011). The sediment composition dominated by reworked littoral carbonates and fauna (mostly fragments of ostracod shelves and pennate diatoms), supports this interpretation. Several processes may have triggered slope instabilities in Lake Montcortès such as slope oversteepening, pore water overpressure, earthquake shaking, or rapid sediment loading identified in other lakes (Locat and Lee, 2002; Sultan et al., 2004; Girardclos et al., 2007; Corella et al., 2013a).

Flood-induced turbidites F-T have thinner sub-layers and their mineralogical composition and terrestrial organic matter suggesting catchment runoff processes. Runoff of sediment-laden currents triggered by extreme rainfall events might have been channelized by reactivating small gullies that are present in the southern area of the lake watershed (Fig. 1B), and reaching distal locations in the lake by hyperpycnal density currents. The faint grading inversions in some of these layers can be attributed to the temporal runoff dynamic (waning and waxing phases) within one hydrological event e.g. (Mulder et al., 2001; Corella et al., 2013a).

5.2- Extreme precipitation intensity reconstruction from instrumental series and detrital microfacies

The relation between washed-in material and storm events can be investigated by correlation between the detrital and the instrumental records. Extreme precipitation mobilizes and entrains sediment available in the watershed which is transported via diffuse runoff or channelized flow into the lake basin and deposited in the lake bottom. M-T and matrix-supported layers deposition are not directly linked to extreme hydrological events.

The different flood-related microfacies types shed light on the magnitude of rainfall events. N.C. DL represent run-off events produced by rainfalls above 80 mm MDP (2-year return period) while FT and DL are associated with rainfalls exceeding 90 mm MDP that occur with an average recurrence interval of four years or longer. This relationship documented in Montcortès highlights the significance of microfacies analyses to evaluate the intensity of rainfall-induced floods.

Layer thickness may be related to flood magnitudes (Schiefer et al., 2006; Schiefer et al., 2011). However, it usually shows a complex nonlinear relation and in some cases a correlation between layer thickness and flood magnitude has just not been observed (Czymzik et al., 2010; Kämpf et al., 2012). In Lake Montcortès the relation between layer thickness and rainfall intensity is also not straightforward because the amount of mobilized sediment may also depend on the sediment availability and its temporal storage in the catchment (Lamoureux, 2000; Czymzik et al., 2010). Nevertheless, in general, thinner layers seem to correspond with rainfall events < 90 mm MDP while the thickest deposits usually correspond with precipitation events > 100 mm MDP (Fig. 5). Most of the MDP maxima are characterized by increases in zirconium except for the AD 1982 extreme precipitation event, where potassium increases (Fig. 5). In Lake Montcortès, zirconium content is directly related to grain-size and microfacies variability (Figs 2 and 3) and could be considered as a proxy for rainfall intensity as particle-size entrained by a flow is also related to the hydraulic energy of the current (Mulder et al., 2001; 2003) and, thus, to flood magnitude.

A reliable assessment of extreme event recurrence rates needs to evaluate the completeness of the detrital layer record (Czymzik et al., 2010; Kämpf et al., 2012). Lake Montcortès has a low sensitivity to rainfall events of 80 - 100 mm MDP of which only 25 % resulted in detrital layer formation compared to 70 % of extreme rainfall events > 100 mm MDP leading to detrital layer deposition in the record. This suggests that 100 mm maximum daily rainfall is a critical threshold for Lake Montcortès. Below that rainfall amount flood layers only occasionally were recorded in the stratigraphic record. The non-continuous nature of N.C. DL should be particularly considered when evaluating the Lake Montcortès completeness, as N.C. DL could have not been deposited at the coring sites and then, their presence can be underestimated.

All of the extreme rainfalls exceeding 110 mm MDP with a return period of 8 years and longer during the instrumental period are recorded in the lake stratigraphy so we expect Lake Montcortès to represent a complete record of such extreme hydrological rainfall events.

5.3- Extreme precipitation and climate variability in NE Iberian Peninsula since 1374

The clastic layers in Lake Montcortès provide a unique record of extreme rainfalls back to the 14th century at an annual scale. In addition, the comparison with instrumental time-series has enabled to assign minimum rainfall threshold values for detrital layer deposition. It is worth noting that these thresholds might have been different in the past when land use conditions in the lake watershed were different. Hence, they should be carefully interpreted in terms of reconstructing past rainfall amplitudes. Distinct periods of low and high extreme hydrological events frequencies and intensities have been distinguished (Fig. 6; Table 2).

Increased extreme rainfall frequency periods (AD 1347-1400 and AD 1844-1894).

Two ca 50 year-long intervals stand out as the periods of most intensive hydrological activity in the region since the 14th century. The first period correspond to the transition from the Medieval Climate Anomaly (MCA, AD 1000 - 1300) to the Little Ice Age (LIA, AD 1450-1850). Several authors have proposed a readjustment of atmospheric circulation patterns in the North Atlantic realm towards a higher frequency of negative NAO modes during that transition that could have resulted in higher extreme rainfall frequency during this phase in western Mediterranean (Trouet et al., 2009; Morellón et al., 2012; Moreno et al., 2012; Trouet et al., 2012). The high sediment delivery to the lake during this period does not seem related to human activities in the lake´s catchment. The anthropogenic pressure in the watershed was considerably low due to the numerous civil wars and the Black Death pandemic in AD 1348 that resulted in a significant depopulation in the region (Marugan and Oliver, 2005; Rull et al., 2011). Pollen data from Montcortès sediments also show that population pressure in the region diminished during the MCA/LIA transition, as indicated by a decreasing trend in meadows/pastures and herbaceous crops and smaller percentages of charcoal (Rull et al., 2011). More intense human activities around the lake did not recovered until the 17th century, marked by an increased in charcoal and *Cannabis*-type pollen.

The second half of the 19th century (AD 1844-1894) highlights the period with strongest extreme precipitation occurrence in terms of frequency and intensity (Table 2). During the beginning of the 19th century the demographic pressure in several Pyrenean mountain valleys increased, followed by a significant population decrease by the end of the century (Fillat et al., 2008). In Montcortès a decline in hemp cultivation and/or retting and a re-expansion of conifer forest occurred after ca AD 1830 (Rull et al., 2011), clearly marking the onset of a population decrease, particularly intensified after

AD 1870 (Farràs, 2005). Anthropogenic influence does not seem to be the main factor for the AD 1844-1894 period of maximum flood layers because human impact in the watershed had already decreased at that time. Moreover, historically described floods in the nearby Segre River and in Catalonian rivers also show a maximum intensity and frequency during this period (Llasat et al., 2005; Barriendos and Rodrigo, 2006). Extreme floods occurred in most rivers in NE Iberian Peninsula during this period (Fig. 6) supporting climate variability as the main cause for this flood period.

The periods with increase in extreme precipitation events occurred at the onset and termination of the LIA, coinciding with a higher flood frequency in the southwestern Alps, e.g. Lake Allos (Wilhelm et al., 2012), and in Mediterranean rivers (Benito et al., 2008; 2010) as well as with significant water level oscillations in other Pyrenean lakes, e.g., Lake Estanya: (Morellón et al., 2009; 2011); Lake Basa de la Mora (Pérez-Sanz et al., 2013), an in the western Ebro Basin (Lake Arreo; Corella et al., 2013b). Interestingly, the increase in intense rainfall events in the western Mediterranean coincides with drier conditions in some eastern Mediterranean lakes suggesting a Mediterranean see-saw pattern during the last centuries (Roberts et al., 2012). Our data supports the hypothesis of increasing frequencies and magnitudes of floods during periods of rapid climate changes, e.g. (Macklin et al., 2006) when changes in atmospheric circulation patterns can result in changes in magnitude and recurrence rates of extreme rainfall and related floods, e.g. (Knox, 2000).

Low rainfall frequency and intensity periods (AD 1441-1508, 1547-1592, 1656-1712, 1765-1822, 1917-2012).

The five periods of low frequency of extreme precipitation are in good agreement with periods of low frequency of historical floods in the Segre River and in other NE Iberian Peninsula rivers (Fig. 6). Low-resolution pollen records from Montcortès sediments do not show significant changes in vegetation cover during those periods except for the period AD 1441-1508, with a forest recovery, and the AD 1765-1822 with a forest contraction (Rull et al. 2011).

A striking feature of the Montcortès record is that the periods of low flood activity coincide with periods of low total solar irradiance TSI (Delaygue and Bard, 2011) (Fig. 6). In particular, the period 1441-1508 with a significant reduction in the number of rainfall events (mean frequency of 0.15 events/year; Table 2) is positively correlated with the lowest solar activity in the last millennium during the Spörer Minimum at around AD 1450. This connection between high (low) solar activity and increase (decrease) in the number of floods reinforces the hypothesis of solar-induced changes in the atmospheric circulation patterns driving precipitation changes in Western Europe. Nevertheless, the physical mechanism behind the solar-climate linkage is still a matter of debate. Previous authors suggested a more negative NAO state during solar lows leading to higher flood frequencies in the Alps (e.g., Czymzik et al., 2013; Wirth et al 2013a, b). However, the opposite trend has been shown in Lake Montcortès as well as in other lake and fluvial records in the Iberian Peninsula (Benito et al., 2003; Vaquero, 2004; Moreno et al., 2008) and western Alps (Wilhelm et al., 2012). These results reflect a strong regional contrast in the occurrence of extreme hydrometeorological events and highlights that the relationship between solar activity and NAO dynamics is not completely understood e.g. (Kirov and Georgieva, 2002).

An outstanding feature of the Montcortès extreme rainfall event record is the 20th century, which is the longest time interval with the low frequency of heavy rainfall events (mean frequency of 0.12 events > 80 mm MDP/year). This scarcity in heavy rainfall since AD 1917 coincides with relatively lower lake levels and higher salinity in other pre-Pyrenean lakes - e.g., Lake Estanya (Morellón et al., 2011), Lake Basa de la

Mora (Pérez-Sanz et al., 2013) and Lake Arreo (Corella et al., 2013b) -. A reduced number of extreme floods during the 20th century were also reported in the southeastern Spanish Mediterranean region (Machado et al., 2011). Changes in the land uses during the second half of the 20th century associated to the documented reduced human pressure in the Pyrenees, particularly intense since 1950s (García-Ruíz, 2010) could have had an impact on the sediment availability and soil erodibility. However, the low number of extreme rainfall events recorded in Lake Montcortès is in agreement with a general decrease in annual precipitation, number of rainy days and precipitation intensity in northeastern Spain during the second half of the 20th century (López-Moreno et al., 2010; Acero et al., 2011).

The uniqueness of the 20th century flood history is more evident when considered that this decrease in extreme rainfall during the second half of the 20th century is at odds with the hypothesis of more extreme rainfall events under a climate scenario of increased summer temperatures and with relatively higher solar irradiance after the end of the LIA. Higher temperature gradients between the Mediterranean and the continent are assumed to lead to an increase in extreme rainfall events due to the rise on moisture-holding capacity of the atmosphere according to the Clausius-Clapeyron formula - 7 % per degree temperature rise (Emori and Brown, 2005). A shift in atmospheric circulation patterns no longer control by TSI is the most plausible explanation for this decrease in extreme precipitation. A change from persistent autumn NAO negative mode during the 19th century towards a dominant positive autumn NAO index during the 20th (Luterbacher et al., 2002) (Fig. 6) could be responsible for lower total annual precipitation in NE Iberian Peninsula in agreement with Lake Montcortès record. This current period of low extreme rainfall event frequency is the longest (85 years) of the record (50-60 years) and it seems to be climate-driven although could have been amplified by human impact in the watershed.

6- CONCLUSIONS

The varved sediments from Lake Montcortès provide, for the first time in the Iberian Peninsula, semiquantitative reconstruction of the intensity of extreme precipitation events since AD 1347. A detailed microfacies characterization and their comparison with instrumental daily precipitation time series since AD 1917 allowed an innovative quantification of two minimum rainfall thresholds leading to detrital layers deposition. About 70% of rainfalls above 100 mm intensity (5-year average return interval) were recorded as flood layers demonstrating that the effectiveness of Lake Montcortès to record heavy rainfalls is sufficient to determine the extreme rainfall frequency with an annual resolution over the last centuries. Two periods with increased rainfall frequency and intensity occurred at the onset and termination of the LIA between AD 1347-1400 and AD 1844-1894 highlighting the hydrological instability during periods of rapid climatic changes. Lower frequency and magnitude of heavy rainfall occur between AD 1441-1508, 1547-1592, 1656-1712, 1765-1822 and 1917-2012. This record constitutes a remarkable example of extreme events recurrence rates estimation beyond the instrumental record using annually laminated natural proxies.

Lake Montcortès reconstruction is in agreement with historical flood reconstructions from NE spanish rivers and other paleohydrological records from the Pyrenees and Western Alps. In addition, the chronological control of the studied record and the semiquantitative nature of the reconstruction improves our understanding of past regional extreme rainfall variability in western Mediterranean areas. Variations in extreme rainfall frequencies prior to the 20th century show a positive correlation with solar activity and autumn reconstructions of the North Atlantic Oscillation, suggesting complex solar induced-changes in atmospheric circulation patterns. The reduction on extreme rainfall frequency since early 20th century has not precedent in the last 600 years, and although perhaps amplified by human impact in the watershed, it does not fit with foreseen regional trends of increasing frequency of extreme rainfalls under anthropogenic climate change.

7- ACKNOWLEDGMENTS

The research conducted in this study was provided by the Spanish Inter-Ministry of Science and Technology (CICYT), through the projects GLOBALKARST (CGL2009-08415), CONSOLIDER-GRACCIE (CSD00C-07-22422) and CLARIES (CGL2011-29176). The EU COST Action ES0907 INTIMATE provided a travel grant to GFZ (Potsdam). Climatic instrumental data are courtesy of the Spanish National Meteorological Agency (AEMET). Juan Pablo Corella holds a JAE-DOC post-doctoral contract co-funded by CSIC and the European Social Fund.

8- REFERENCES

Acero, F.J., García, J.A., Gallego, M.C., 2011. Peaks-over-threshold study of trends in extreme rainfall over the Iberian Peninsula. Journal of Climate 24, 1089-1105.

Appleby, P.G., 2001. Chronostratigraphic techniques in recent sediments, in: Last, W.M., Smol, J.P. (Eds.), Tracking Environmental Change Using Lake Sediments. Volume 1: Basin Analysis, Coring, and Chronological Techniques. Kluwer Academic Publishers, Dordrecht, pp. 171-203.

Arnaud, F., Lignier, V., Revel, M., Desmet, M., Beck, C., Pourchet, M., Charlet, F., Trentesaux, A., Tribovillard, N., 2002. Flood and earthquake disturbance of 210Pb geochronology (Lake Anterne, NW Alps). Terra Nova 14, 225-232.

Baker, V.R., 2008. Paleoflood hydrology: Origin, progress, prospects. Geomorphology 101, 1-13.

Barriendos, M., Rodrigo, F.S., 2006. Study of historical flood events on Spanish rivers using documentary data. Hydrological Sciences Journal 51, 765-783.

Benito, G., Díez-Herrero, A., Fernández de Villalta, M., 2003. Magnitude and frequency of flooding in the Tagus basin (Central Spain) over the last millennium. Climatic Change 58, 171-192.

Benito, G., Machado, M.J., Pérez-González, A., 1996. Climate change and flood sensitivity in Spain, in: Branson, J., Brown, A.G., Gregory, K.J. (Eds.), Global continental changes: the context of paleohydrology. The Geological Society of London, London, pp. 85-98.

Benito, G., Thorndycraft V.R., Rico M., Sánchez-Moya Y., Sopeña A., 2008. Palaeoflood and floodplain records from Spain: Evidence for long-term climate variability and environmental changes. Geomorphology, 101, 68–77.

Benito, G., Rico M., Sánchez-Moya Y. Sopeña, Thorndycraft V. R., Barriendos, M,. 2010. The impact of late Holocene climatic variability and land use change on the flood hydrology of the Guadalentín River, southeast Spain. Global and Planetary Change 70, 53–63.

Benito, G., O´Connor, J.E., 2013. Quantitative Paleoflood Hydrology, in: Shroder, J.F., Wohl, E. (Eds.), Treatise on Geomorphology, Vol 9, Fluvial Geomorphology. Academic Press, San Diego, pp. 459-474.

Bentabol, H., 1900. Las Aguas de España y Portugal.

Brauer, A., Casanova, J., 2001. Chronology and depositional processes of the laminated sediment record from Lac d'Annecy, French Alps. Journal of Paleolimnology 25, 163–177.

Brauer, A., Mangili, C., Moscariello, A., Witt, A., 2008. Palaeoclimatic implications from micro-facies data of a 5900 varve time series from the Piànico interglacial sediment record, southern Alps. Palaeogeography, Palaeoclimatology, Palaeoecology 259, 121-135.

Bussmann, F., Anselmetti, F., 2010. Rossberg landslide history and flood chronology as recorded in Lake Lauerz sediments (Central Switzerland). Swiss Journal of Geosciences 103, 43-59.

Comisión Técnica de Inundaciones, C.T.d., 1985a. Estudio de Inundaciones Históricas: Mapa de Riesgos Potenciales. Cuenca del Ebro. Comisión Nacional de Protección Civil, Madrid.

Comisión Técnica de Inundaciones, C.T.d., 1985b. Estudio de Inundaciones Históricas: Mapa de Riesgos Potenciales. Cuenca del Pirineo Oriental. Comisión Nacional de Protección Civil, Madrid, Madrid.

Corella, J.P., Arantegui, A., Loizeau, J.L., DelSontro, T., le Dantec, N., Stark, N., Anselmetti, F., Girardclos, S., 2013a. Sedyment dynamics in the subaquatic channel of the Rhone delta (Lake Geneva, France/Switzerland). Aquatic Sciences - Research Across Boundaries.

Corella, J.P., Stefanova, V., El Anjoumi, A., Rico, E., Giralt, S., Moreno, A., Plata-Montero, A., Valero-Garcés, B.L., 2013b. A 2500-year multi-proxy reconstruction of climate change and human activities in northern Spain: The Lake Arreo record. Palaeogeography, Palaeoclimatology, Palaeoecology 386, 555-568.

Corella, J.P., Brauer, A., Mangili, C., Rull, V., Vegas-Vilarrúbia, T., Morellón, M., Valero-Garcés, B.L., 2012. The 1.5-ka varved record of Lake Montcortès (southern Pyrenees, NE Spain). Quaternary Research 78, 323-332.

Corella, J.P., Moreno, A., Morellón, M., Rull, V., Giralt, S., Rico, M.T., Pérez-Sanz, A., Valero-Garcés, B.L., 2011. Climate and human impact on a meromictic lake during the last 6,000 years (Montcortès Lake, Central Pyrenees, Spain). Journal of Paleolimnology 46, 351-367.

Cuven, S., Francus, P., Lamoureux, S.F., 2010. Estimation of grain size variability with micro X-ray fluorescence in laminated lacustrine sediments, Cape Bounty, Canadian High Arctic. Journal of Paleolimnology 44, 803-817.

Czymzik, M., Brauer, A., Dulski, P., Plessen, B., Naumann, R., von Grafenstein, U., Scheffler, R., 2013. Orbital and solar forcing of shifts in Mid- to Late Holocene flood intensity from varved sediments of pre-alpine Lake Ammersee (southern Germany). Quaternary Science Reviews 61, 96-110.

Czymzik, M., Dulski, P., Plessen, B., von Grafenstein, U., Naumann, R., Brauer, A., 2010. A 450 year record of spring-summer flood layers in annually laminated sediments from Lake Ammersee (southern Germany). Water Resources Research 46, W11528.

Debret, M., Chapron, E., Desmet, M., Rolland-Revel, M., Magand, O., Trentesaux, A., Bout-Roumazeille, V., Nomade, J., Arnaud, F., 2010. North western Alps Holocene paleohydrology recorded by flooding activity in Lake Le Bourget, France. Quaternary Science Reviews 29, 2185-2200.

Delaygue, G., Bard, E., 2011. An Antarctic view of Beryllium-10 and solar activity for the past millennium. Climate Dynamics 36, 2201-2218.

Emori, S., Brown, S.J., 2005. Dynamic and thermodynamic changes in mean and extreme precipitation under changed climate. Geophysical Research Letters 32, L17706.

Etoh, T., Murota, A., Nakanishi, M., 1987. SQRT-Exponential Type Distribution of Maximum, in: Singh, V. (Ed.), Hydrologic Frequency Modeling. Springer Netherlands, pp. 253-264.

Farràs, F., 2005. El Pallars contemporani, in: Marguan, C.M.R., V. (eds,) (Ed.), Història del Pallars. Dels orígens als nostre dies. . Pagès Editors, Lleida, pp. 121-144.

Fillat, F., García-González, R., Gómez, D., Reiné, R., 2008. Pastos del Pirineo. Consejo Superior de Investigaciones Científicas (C.S.I.C), Madrid, Spain.

Font, I., 1988. Historia del Clima en España. Cambios Climáticos y sus Causas, Madrid.

Fontana-Tarrats, J.M., 1976. Historia del Clima en Cataluña. Noticias, Madrid.

García-Ruiz, J.M., 2010. The effects of land uses on soil erosion in Spain: a review. Catena 81, 1–11.

Giguet-Covex, C., Arnaud, F., Enters, D., Poulenard, J., Millet, L., Francus, P., David, F., Rey, P.-J., Wilhelm, B., Delannoy, J.-J., 2012. Frequency and intensity of high-altitude floods over the last 3.5 ka in northwestern French Alps (Lake Anterne). Quaternary Research 77, 12-22.

Gilli, A., Anselmetti, F., Ariztegui, D., McKenzie, J., 2003. A 600-year sedimentary record of flood events from two sub-alpine lakes (Schwendiseen, Northeastern Switzerland), Lake Systems from the Ice Age to Industrial Time. Birkhäuser Basel, pp. 49-58.

Gilli, A., Anselmetti, F., Glur, L., Wirth, S., 2013. Lake Sediments as Archives of Recurrence Rates and Intensities of Past Flood Events, in: Schneuwly-Bollschweiler, M., Stoffel, M., Rudolf-Miklau, F. (Eds.), Dating Torrential Processes on Fans and Cones. Springer Netherlands, pp. 225-242.

Girardclos, S., Schmidt, O.T., Sturm, M., Ariztegui, D., Pugin, A., Anselmetti, F.S., 2007. The 1996 AD delta collapse and large turbidite in Lake Brienz. Marine Geology 241, 137-154.

Gorsline, D.S., De Diego, T., Nava-Sanchez, E.H., 2000. Seismically triggered turbidites in small margin basins: Alfonso Basin, Western Gulf of California and Santa Monica Basin, California Borderland. Sedimentary Geology 135, 21-35.

Hattermann, F.F., Kundzewicz, Z.W., Huang, S., Vetter, T., Kron, W., Burghoff, O., Merz, B., Bronstert, A., Krysanova, V., Gerstengarbe, F.-W., Werner, P., Hauf, Y., 2012. Flood risk from a holistic perspective -observed changes in Germany, in: Kundzewicz, Z.W. (Ed.), Changes in Flood Risk in Europe. CRC Press, Wallingford, UK, pp. 212-237.

Hartmann, D.L., Klein Tank, A.M.G., Rusticucci, M., Alexander, L.V., Brönnimann, S., Charabi, Y., Dentener, F.J., Dlugokencky, E.J., Easterling, D.R., Kaplan, A., Soden, B.J., Thorne, P.W., Wild M., Zhai, P.M., 2013. Observations: Atmosphere and Surface. In: Climate Change 2013: The Physical Science Basis. Contribution of Working Group I to the Fifth Assessment Report of the Intergovernmental Panel on Climate Change [Stocker, T.F., D. Qin, G.-K. Plattner, M. Tignor, S.K. Allen, J. Boschung, A. Nauels, Y. Xia, V. Bex and P.M. Midgley (eds.)]. Cambridge University Press, Cambridge, United Kingdom and New York, NY, USA, pp. 159-254.

Kämpf, L., Brauer, A., Dulski, P., Lami, A., Marchetto, A., Gerli, S., Ambrosetti, W., Guilizzoni, P., 2012. Detrital layers marking flood events in recent sediments of Lago Maggiore (N. Italy) and their comparison with instrumental data. Freshwater Biology 57, 2076-2090.

Karlin, R.E., Holmes, M., Abella, S., Sylwester, R., 2004. Holocene landslides and a 3500-year record of Pacific Northwest earthquakes from sediments in Lake Washington. Geological Society of America Bulletin 116, 94-108.

Kirov, B., Georgieva, K., 2002. Long term variations and interrelations of ENSO, NAO and solar activity. Physics and Chemistry of the Earth 27, 441–448.

Knox, J.C., 1985. Responses of floods to Holocene climatic change in the upper Mississippi Valley. Quaternary Research 23, 287-300.

Knox, J.C., 2000. Sensitivity of modern and Holocene floods to climate change. Quaternary Science Reviews 19, 439-457.

Kundzewicz, Z.W., Kanae, S., Seneviratne, S.I., Handmer, J., Nicholls, N., Peduzzi, P., Mechler, R., Bouwer, L.M., Arnell, N., Mach, K., Muir-Wood, R., Brakenridge, G.R., Kron, W., Benito, G., Honda, Y., Takahashi, K., Sherstyukov, B., 2014. Flood risk and climate change: global and regional perspectives. Hydrological Sciences Journal 59, 1-28.

Kyselý, J., 2009. Trends in heavy precipitation in the Czech Republic over 1961–2005. International Journal of Climatology 29, 1745-1758.

Lamoureux, S., 2000. Five centuries of interannual sediment yield and rainfall-induced erosion in the Canadian High Arctic recorded in lacustrine varves. Water Resources Research 36, 309-318.

Locat, J., Lee, H.J., 2002. Submarine landslides: advances and challenges. Canadian Geotechnical Journal 39, 193-212.

López-Bustos, A., 1981. Tomando el Pulso a las Grandes Crecidas de los Ríos Peninsulares. Revista Obras Públicas, 179-192.

López-Moreno, J.I., Vicente-Serrano, S.M., Angulo-Martínez, M., Beguería, S., Kenawy, A., 2010. Trends in daily precipitation on the northeastern Iberian Peninsula, 1955–2006. International Journal of Climatology 30, 1026-1041.

Luterbacher, J., Xoplaki, E., Dietrich, D., Rickli, R., Jacobeit, J., Beck, C., Gyalistras, D., Schmutz, C., Wanner, H., 2002. Reconstruction of sea level pressure fields over the Eastern North Atlantic and Europe back to 1500. Climate Dynamics 18, 545-561.

Llasat, M.C., Barriendos, M., Barrera, A., Rigo, T., 2005. Floods in Catalonia (NE Spain) since the 14th century. Climatological and meteorological aspects from historical documentary sources and old instrumental records. Journal of Hydrology 313, 32-47.

Llasat, M.C., Puigcerver, M., 1994. Meteorological Factors Associated with Floods in the North-Eastern Part of the Iberian Peninsula, in: El-Sabh, M.I., Murty, T.S., Venkatesh, S., Siccardi, F., Andah, K. (Eds.), Recent Studies in Geophysical Hazards. Springer Netherlands, pp. 81-93.

Macklin, M.G., Benito, G., Gregory, K.J., Johnstone, E., Lewin, J., Michczyñska, D.J., Soja, R., Starkel, L., Thorndycraft, V.R., 2006. Past hydrological events reflected in the Holocene fluvial record of Europe. Catena 66, 145-154.

Machado, M.J., Benito, G., Barriendos, M., Rodrigo, F.S., 2011. 500 Years of rainfall variability and extreme hydrological events in southeastern Spain drylands. Journal of Arid Environments 75, 1244-1253.

Mangili, C., Brauer, A., Moscariello, A., Naumann, R., 2005. Microfacies of detrital event layers deposited in Quaternary varved lake sediments of the Piànico-Sèllere Basin (northern Italy). Sedimentology 52, 927-943.

Martin-Puertas, C., Matthes, K., Brauer, A., Muscheler, R., Hansen, F., Petrick, C., Aldahan, A., Possnert, G., van Geel, B., 2012. Regional atmospheric circulation shifts induced by a grand solar minimum. Nature Geosci 5, 397-401.

Martin-Vide, J., Sanchez-Lorenzo, A., Lopez-Bustins, J.A., Cordobilla, M.J., Garcia-Manuel, A., Raso, J.M., 2008. Torrential Rainfall in Northeast of the Iberian Peninsula: Synoptic patterns and WeMO influence. Advances in Science and Research 2, 99-105.

Marugan, C.M., Oliver, J., 2005. El Pallars medieval, in: Marguan, C.M.R., V. (eds,) (Ed.), Història del Pallars. Dels orígens als nostre dies. Pagès Editors, Lleida, pp. 45-86.

Masachs, V., 1948. El Régimen de los Ríos Peninsulares. CSIC, Barcelona.

Masachs, V., 1950. Aportación al Conocimiento del Régimen Fluvial Mediterráneo, Comptes Rendus du Congrès International de Géographie, UGI, II, Lisbonne, pp. 358-390.

Min, S.-K., Zhang, X., Zwiers, F.W., Hegerl, G.C., 2011. Human contribution to more-intense precipitation extremes. Nature 470, 378-381.

Morellón M, Valero-Garcés B, Rico M, Mata P, Delgado-Huertas A, Ó, R., 2009. Evolución sedimentaria y geoquímica del Lago de Estanya (Huesca) durante los últimos 21.000 años. Geogaceta.

Morellón, M., Pérez-Sanz, A., Corella, J.P., Büntgen, U., Catalán, J., González-Sampériz, P., González-Trueba, J.J., López-Sáez, J.A., Moreno, A., Pla-Rabes, S., Saz-Sánchez, M.A., Scussolini, P., Serrano, E., Steinhilber, F., Stefanova, V., Vegas-Vilarrúbia, T., Valero-Garcés, B., 2012. A multi-proxy perspective on millennium-long climate variability in the Southern Pyrenees. Climate of the Past 8, 683-700.

Morellón, M., Valero-Garcés, B., González-Sampériz, P., Vegas-Vilarrúbia, T., Rubio, E., Rieradevall, M., Delgado-Huertas, A., Mata, P., Romero, Ó., Engstrom, D., López-Vicente, M., Navas, A., Soto, J., 2011. Climate changes and human activities recorded in the sediments of Lake Estanya (NE Spain) during the Medieval Warm Period and Little Ice Age. Journal of Paleolimnology 46, 423-452.

Moreno, A., Pérez, A., Frigola, J., Nieto-Moreno, V., Rodrigo-Gámiz, M., Martrat, B., González-Sampériz, P., Morellón, M., Martín-Puertas, C., Corella, J.P., Belmonte, Á., Sancho, C., Cacho, I., Herrera, G., Canals, M., Grimalt, J.O., Jiménez-Espejo, F., Martínez-Ruiz, F., Vegas-Vilarrúbia, T., Valero-Garcés, B.L., 2012. The Medieval Climate Anomaly in the Iberian Peninsula reconstructed from marine and lake records. Quaternary Science Reviews 43, 16-32.

Moreno, A., Valero-Garcés, B.L., González-Sampériz, P., Rico, M., 2008. Flood response to rainfall variability during the last 2000 years inferred from the Taravilla Lake record (Central Iberian Range, Spain). Journal of Paleolimnology DOI 10.1007/s10933-008-9209-3.

Mulder, T., Migeon, S., Savoye, B., Faugeres, J.-C., 2001. Inversely graded turbidite sequences in the deep Mediterranean: a record of deposits from flood-generated turbidity currents? Geo-Marine Letters 21, 86-93.

Mulder, T., Syvitski, J.P., 1995. Turbidity currents generated at river mouths during exceptional discharges to the world oceans. The Journal of Geology 103, 285-299.

Mulder, T., Syvitski, J.P.M., Migeon, S., Faugères, J.-C., Savoye, B., 2003. Marine hyperpycnal flows: initiation, behavior and related deposits. A review. Marine and Petroleum Geology 20, 861-882.

Noren, A.J., Bierman, P.R., Steig, E.J., Lini, A., Southon, J., 2002. Millennial-scale storminess variability in the northeast United States during the Holocene epoch. Nature 419, 821-824.

Ojala, A.E.K., Francus, P., Zolitschka, B., Besonen, M., Lamoureux, S.F., 2012. Characteristics of sedimentary varve chronologies – A review. Quaternary Science Reviews 43, 45-60.

Osleger, D.A., Heyvaert, A.C., Stoner, J.S., Verosub, K.L., 2009. Lacustrine turbidites as indicators of Holocene storminess and climate: Lake Tahoe, California and Nevada. Journal of Paleolimnology 42, 103-122.

Pérez-Sanz, A., González-Sampériz, P., Moreno, A., Valero-Garcés, B., Gil-Romera, G., Rieradevall, M., Tarrats, P., Lasheras-Álvarez, L., Morellón, M., Belmonte, A., Sancho, C., Sevilla-Callejo, M., Navas, A., 2013. Holocene climate variability, vegetation dynamics and fire regime in the central Pyrenees: the Basa de la Mora sequence (NE Spain). Quaternary Science Reviews 73, 149-169.

Rico Sinobas, M., 1850. Fenómenos Meteorológicos en la Península Ibérica desde el Siglo IV hasta el XIX. Real Academia de Medicina de Madrid, Manuscritos 23, 4-15.

Roberts, N., Moreno, A., Valero-Garcés, B.L., Corella, J.P., Jones, M., Allcock, S., Woodbridge, J., Morellón, M., Luterbacher, J., Xoplaki, E., Türkeş, M., 2012. Palaeolimnological evidence for an east–west climate see-saw in the Mediterranean since AD 900. Global and Planetary Change 84–85, 23-34.

Rull, V., González-Sampériz, P., Corella, J., Morellón, M., Giralt, S., 2011. Vegetation changes in the southern Pyrenean flank during the last millennium in relation to climate and human activities: the Montcortès lacustrine record. Journal of Paleolimnology 46, 387-404.

Schiefer, E., Gilbert, R., Hassan, M.A., 2011. A lake sediment-based proxy of floods in the Rocky Mountain Front Ranges, Canada. Journal of Paleolimnology 45, 137-149.

Schiefer, E., Menounos, B., Slaymaker, O., 2006. Extreme sediment delivery events recorded in the contemporary sediment record of a montane lake, southern Coast Mountains, British Columbia. Canadian Journal of Earth Sciences 43, 1777-1790.

Scussolini, P., Vegas-Vilarrúbia, T., Rull, V., Corella, J., Valero-Garcés, B., Gomà, J., 2011. Middle and late Holocene climate change and human impact inferred from diatoms, algae and aquatic macrophyte pollen in sediments from Lake Montcortès (NE Iberian Peninsula). Journal of Paleolimnology 46, 369-385.

Seneviratne, S.I., Nicholls, N., Easterling, D., Goodess, C.M., Kanae, S., Kossin, J., Luo, Y., Marengo, J., McInnes, K., Rahimi, M., M. Reichstein, M., Sorteberg, A., Vera, C., Zhang, X., 2012. Changes in climate extremes and their impacts on the natural physical environment, Managing the Risks of Extreme Events and Disasters to Advance Climate Change Adaptation [Field, C.B., V. Barros, T.F. Stocker, D. Qin, D.J. Dokken, K.L. Ebi, M.D. Mastrandrea, K.J. Mach, G.-K. Plattner, S.K. Allen, M. Tignor, and P.M. Midgley (eds.)]. A Special Report of Working Groups I and II of the Intergovernmental Panel on Climate Change (IPCC). Cambridge University Press, Cambridge, UK, and New York, NY, USA, pp. 109-230.

Sturm, M., Matter, A., 1978. Turbidites and varves in Lake Brienz (Switzerland): deposition of clastic detritus by density currents. Special Publications of the International Association of Sedimentologists 2, 147–168.

Sturm, M., Siegenthaler, C., Pickrill, R., 1995. Turbidites and ‘homogenites’, A conceptual model of flood and slide deposits. In „IAS 16th Regional European Meeting, p. 170.

Sultan, N., Cochonat, P., Canals, M., Cattaneo, A., Dennielou, B., Haflidason, H., Laberg, J.S., Long, D., Mienert, J., Trincardi, F., Urgeles, R., Vorren, T.O., Wilson, C., 2004. Triggering mechanisms of slope instability processes and sediment failures on continental margins: a geotechnical approach. Marine Geology 213, 291-321.

Swierczynski, T., Brauer, A., Lauterbach, S., Martín-Puertas, C., Dulski, P., von Grafenstein, U., Rohr, C., 2012. A 1600 yr seasonally resolved record of decadal-scale flood variability from the Austrian Pre-Alps. Geology 40, 1047-1050.

Swierczynski, T., Lauterbach, S., Dulski, P., Delgado, J., Merz, B., Brauer, A., 2013. Mid- to late Holocene flood frequency changes in the northeastern Alps as recorded in varved sediments of Lake Mondsee (Upper Austria). Quaternary Science Reviews 80, 78-90.

Thorndycraft, V.R., Benito, G., Gregory, K.J., 2008. Fluvial geomorphology: A perspective on current status and methods. Geomorphology 98, 2-12.

Toreti, A., Xoplaki, E., Maraun, D., Kuglitsch, F.G., Wanner, H., Luterbacher, J., 2010. Characterisation of extreme winter precipitation in mediterranean coastal sites and associated anomalous atmospheric circulation patterns. Natural Hazards and Earth System Science 10, 1037-1050.

Trouet, V., Esper, J., Graham, N.E., Baker, A., Scourse, J.D., Frank, D.C., 2009. Persistent Positive North Atlantic Oscillation Mode Dominated the Medieval Climate Anomaly. Science 324, 78-80.

Trouet, V., Scourse, J.D., Raible, C.C., 2012. North Atlantic storminess and Atlantic Meridional Overturning Circulation during the last Millennium: Reconciling contradictory proxy records of NAO variability. Global and Planetary Change 84–85, 48-55.

Vanniere et al., 2013. Orbital changes, variation in solar activity and increased anthropogenic activities: controls on the Holocene flood frequency in the Lake Ledro area, Northern Italy Clim. Past, 9, 1193–1209

Vaquero, J.M., 2004. Solar signals in the number of floods recorded for the Tagus river basin over the last millennium. Climatic Change 66, 23-26.

Vicente-Serrano, S.M., Beguería, S., López-Moreno, J.I., El Kenawy, A.M., Angulo-Martínez, M., 2009. Daily atmospheric circulation events and extreme precipitation risk in northeast Spain: Role of the North Atlantic Oscillation, the Western Mediterranean

Oscillation, and the Mediterranean Oscillation. Journal of Geophysical Research: Atmospheres 114, D08106

Wilhelm, B., Arnaud, F., Sabatier, P., Crouzet, C., Brisset, E., Chaumillon, E., Disnar, J.-R., Guiter, F., Malet, E., Reyss, J.-L., Tachikawa, K., Bard, E., Delannoy, J.-J., 2012. 1400 years of extreme precipitation patterns over the Mediterranean French Alps and possible forcing mechanisms. Quaternary Research 78, 1-12.

Wirth, S.B., Gilli, A., Simonneau, A., Ariztegui, D., Vannière, B., Glur, L., Chapron, E., Magny, M., Anselmetti, F.S., 2013a. A 2000-year long seasonal record of floods in the southern European Alps. Geophysical Research Letters 40, 4025-4029.

Wirth, S.B., Glur, L., Gilli, A., Anselmetti, F.S., 2013b. Holocene flood frequency across the Central Alps - solar forcing and evidence for variations in North Atlantic atmospheric circulation. Quaternary Science Reviews 80, 112-128.

Wirth, S.B., Girardclos, S., Rellstab, C., Anselmetti, F.S., 2011. The sedimentary response to a pioneer geo-engineering project: Tracking the Kander River deviation in the sediments of Lake Thun (Switzerland). Sedimentology 58, 1737-1761.

Zolina, O., Simmer, C., Kapala, A., Bachner, S., Gulev, S., Maechel, H., 2008. Seasonally dependent changes of precipitation extremes over Germany since 1950 from a very dense observational network. Journal of Geophysical Research D: Atmospheres 113.

FIGURE CAPTIONS

Figure 1. (1A) Location of Lake Montcortès in the Iberian Peninsula and Digital Terrain Model (resolution 5m) of the Pallars Sobira region and location of Lake Montcortès, Segre River and Cabdella meteorological station. (1B) Land use map -Corine, (EEA, 2000)- of Lake Montcortès catchment area. (1C) Geological map of the watershed (modified from (Rosell, 1994))(1D) 2013 aerial photograph of the Lake Montcortès drainage basin. (1E) Bathymetric map of Lake Montcortès and coring sites.

Figure 2. (Top) Polarized microscope photos of detrital microfacies: A) biogenic varve with absence of clastic layer; B) Non-continuous detrital layer; C) Continuous detrital layer; D) Matrix-supported layer. (Bottom) Thin section scans and XRF photographs of two turbidite types in Lake Montcortès: E) Flood-related turbidite (F-T); F) Mass-movement related turbidite (M-T). Zr, K and Ca/K µ-XRF profiles along the two different turbidites are also shown.

Figure 3. µ-X-ray Fluorescence (XRF) selected elements measured by the core-scanner. From left to right: Core image for the composite sequence for Lake Montcortès record; sedimentary units; K: potassium; Zr: Zirconium; Ca/K: Calcium-potassium ratio; TOC: Total Organic Carbon; Ca: Calcium; TIC: Total Inorganic Carbon

Figure 4. Core image and resulting age-depth model based on varve counting and ^{210}Pb radiometric dating. The unsupported lead activities are shown in the upper right panel –Dates shown in gray (unit II) are not considered for the age model -. The radiocarbon date was obtained of aquatic organic matter in a different core (MON-04-1A-1K) and correlated with the new sediment cores by identification of key horizons after visual observations and inspection of thin sections.

Figure 5. A) Annual dairy maximum precipitation Versus thickness and occurrence of the different detrital microfacies. Historical floods in the nearby Segre river are indicated with a star. K and Zr µ-XRF data (cts/s) as indicator of DL and TF respectively. C) Extreme events return period in the area – Detrital microfacies for the period 1917-1994 are also indicated –

Figure 6. Flood reconstruction from NE Iberian Peninsula based on lake and documentary records. From bottom to top: Layer thickness of the different microfacies shown in this study in Lake Montcortès; zirconium (Zr). Flood events/year in Lake Montcortès and 31 yr running average (the red line shows only DL and FT occurrence – more intense precipitation -); Historical floods in Segre and Catalonian rivers

from documentary sources and the spatial distribution of the floods based on the number of river basins affected by the floods; Total solar irradiance (Delaygue and Bard, 2011); Autumn NAO reconstruction (Luterbacher, 2002)

Figure 1. (1A) Location of Lake Montcortès in the Iberian Peninsula and Digital Terrain Model (resolution 5m) of the Pallars Sobira region and location of Lake Montcortès, Segre River and Cabdella meteorological station. (1B) Land use map -Corine, (EEA, 2000)- of Lake Montcortès catchment area (1C) Geological map of the watershed (modified from (Rosell, 1994)). (1D) Aerial photograph of the watershed. (1E) Bathymetric map of Lake Montcortès and coring sites.

Figure 2. (Top) Polarized microscope photos of detrital microfacies: A) biogenic varve with absence of clastic layer; B) Non-continuous detrital layer; C) Continuous detrital layer; D) Matrix-supported layer. (Bottom) Thin section scans and XRF photographs of two turbidite types in Lake Montcortès: E) Flood-related turbidite (F-T); F) Mass-movement related turbidite (M-T). Zr, K and Ca/K µ-XRF profiles along the two different turbidites are also shown.

Figure 3. µ-X-ray Fluorescence (XRF) selected elements measured by the core-scanner. From left to right: Core image for the composite sequence for Lake Montcortès record; sedimentary units; K: potassium; Zr: Zirconium; Ca/K: Calcium-potassium ratio; TOC: Total Organic Carbon; Ca: Calcium; TIC: Total Inorganic Carbon

Figure 4. Core image and resulting age-depth model based on varve counting and ^{210}Pb radiometric dating. The unsupported lead activities are shown in the upper right panel –Dates shown in gray (unit II) are not considered for the age model -. The radiocarbon date was obtained of aquatic organic matter in a different core (MON-04-1A-1K) and correlated with the new sediment cores by identification of key horizons after visual observations and inspection of thin sections.

Figure 5. A) Annual dairy maximum precipitation Versus thickness and occurrence of the different detrital microfacies. Historical floods in the nearby Segre river are indicated with a star. K and Zr µ-XRF data (cts/s) as indicator of DL and TF respectively. C) Extreme events return period in the area – Detrital microfacies for the period 1917-1994 are also indicated –

Figure 6. Flood reconstruction from NE Iberian Peninsula based on lake and documentary records. From bottom to top: Layer thickness of the different microfacies shown in this study in Lake Montcortès; zirconium (Zr). Flood events/year in Lake Montcortès and 31 yr running average (the red line shows only DL and FT occurrence – more intense precipitation -); Historical floods in Segre and Catalonian rivers from documentary sources and the spatial distribution of the floods based on the number of river basins affected by the floods. Total solar irradiance (Delaygue and Bard, 2011)

1016

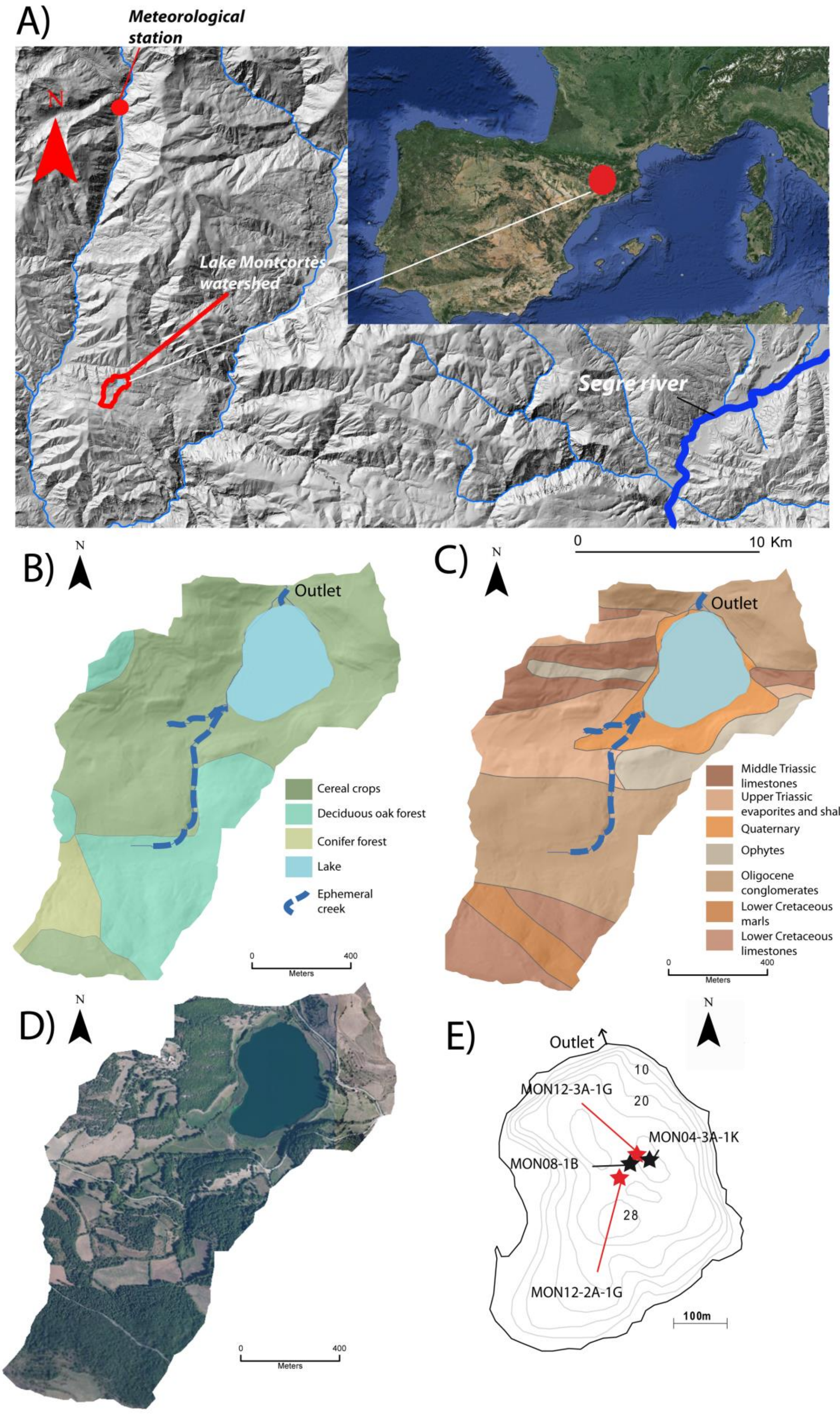
A)
Meteorological station
N
Lake Montcortès watershed
Segre river
0
10 Km
B)
N
Outlet
Cereal crops
Deciduous oak forest
Conifer forest
Lake
Ephemeral creek
0
400
Meters
C)
N
Outlet
Middle Triassic limestones
Upper Triassic evaporites and shales
Quaternary
Ophytes
Oligocene conglomerates
Lower Cretaceous marls
Lower Cretaceous limestones
0
400
Meters
D)
N
0
400
Meters
E)
N
Outlet
10
20
28
MON12-3A-1G
MON04-3A-1K
MON08-1B
MON12-2A-1G
100m

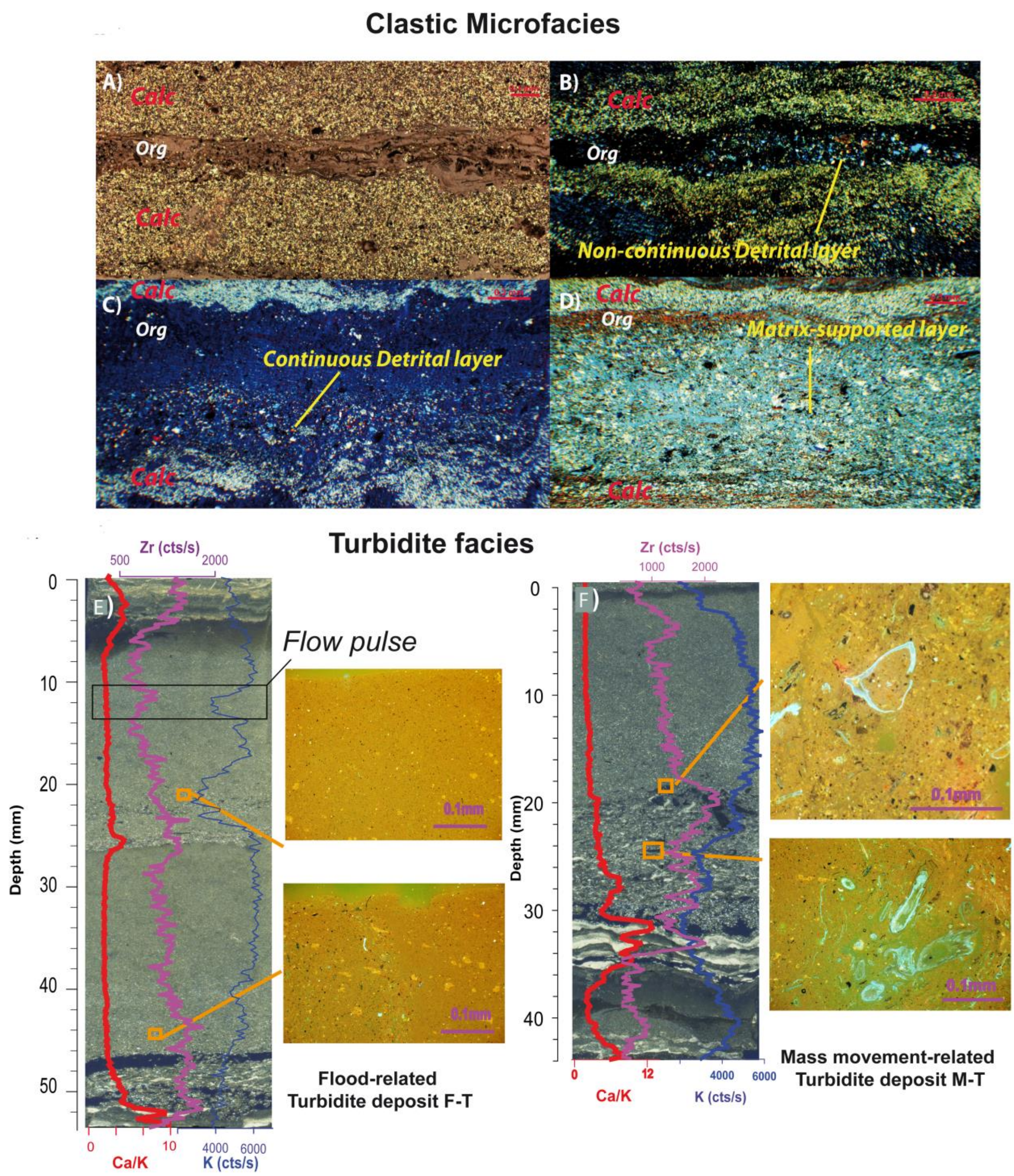
Clastic Microfacies
A)
Calc
Org
Calc
B)
Calc
Org
Non-continuous Detrital layer
C)
Calc
Org
Continuous Detrital layer
Calc
D)
Calc
Org
Matrix-supported layer
Calc
Turbidite facies
Zr (cts/s)
500
2000
E)
Flow pulse
0.1mm
0.1mm
Depth (mm)
0
10
20
30
40
50
0
10
4000
6000
Ca/K
K (cts/s)
Flood-related
Turbidite deposit F-T
Zr (cts/s)
1000
2000
F)
Depth (mm)
0
10
20
30
40
0
12
4000
6000
Ca/K
K (cts/s)
0.1mm
0.1mm
Mass movement-related
Turbidite deposit M-T

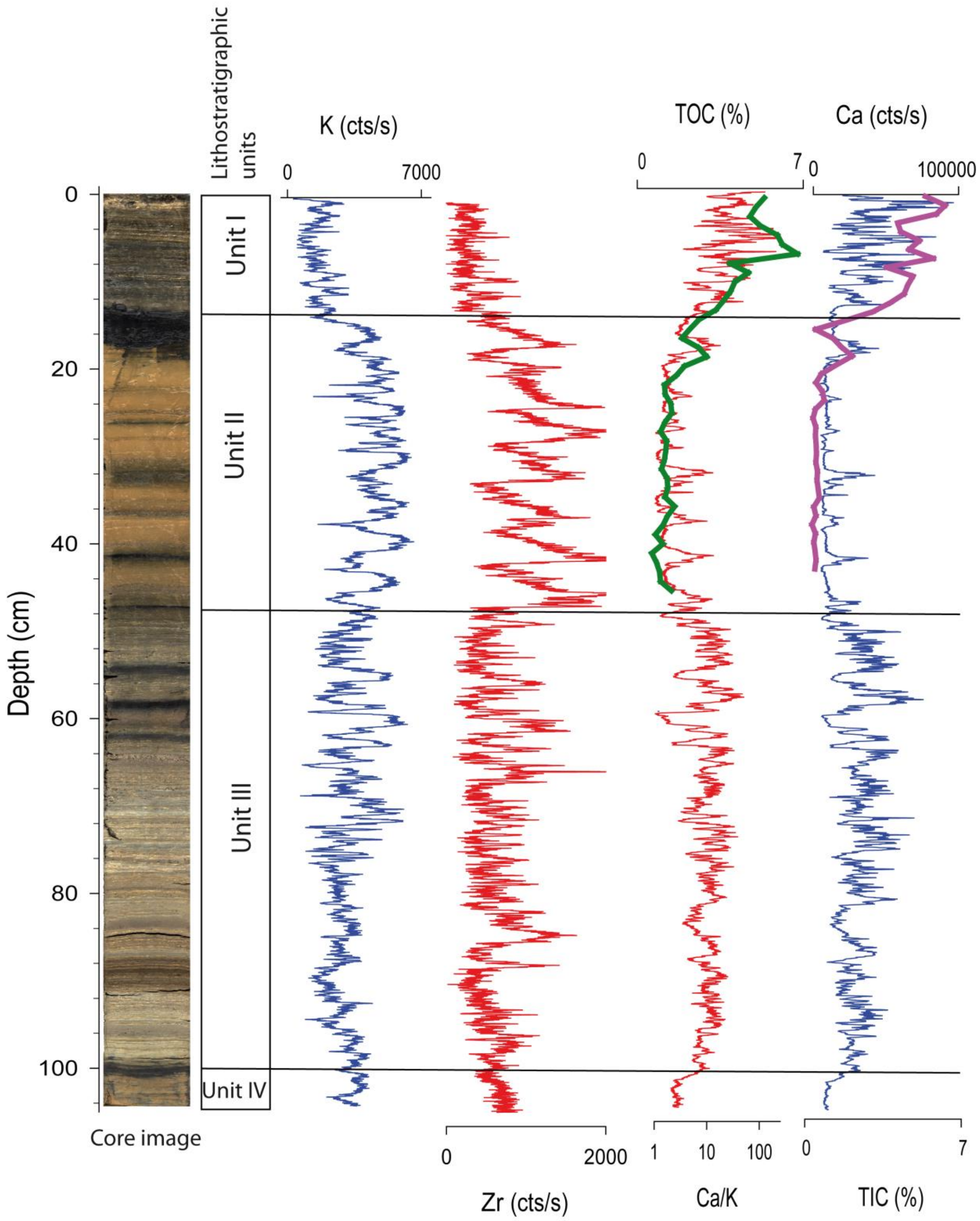
Lithostratigraphic units
K (cts/s)
0
7000
TOC (%)
0
7
Ca (cts/s)
0
100000
Depth (cm)
0
20
40
60
80
100
Unit I
Unit II
Unit III
Unit IV
Core image
Zr (cts/s)
0
2000
Ca/K
1
10
100
TIC (%)
0
7

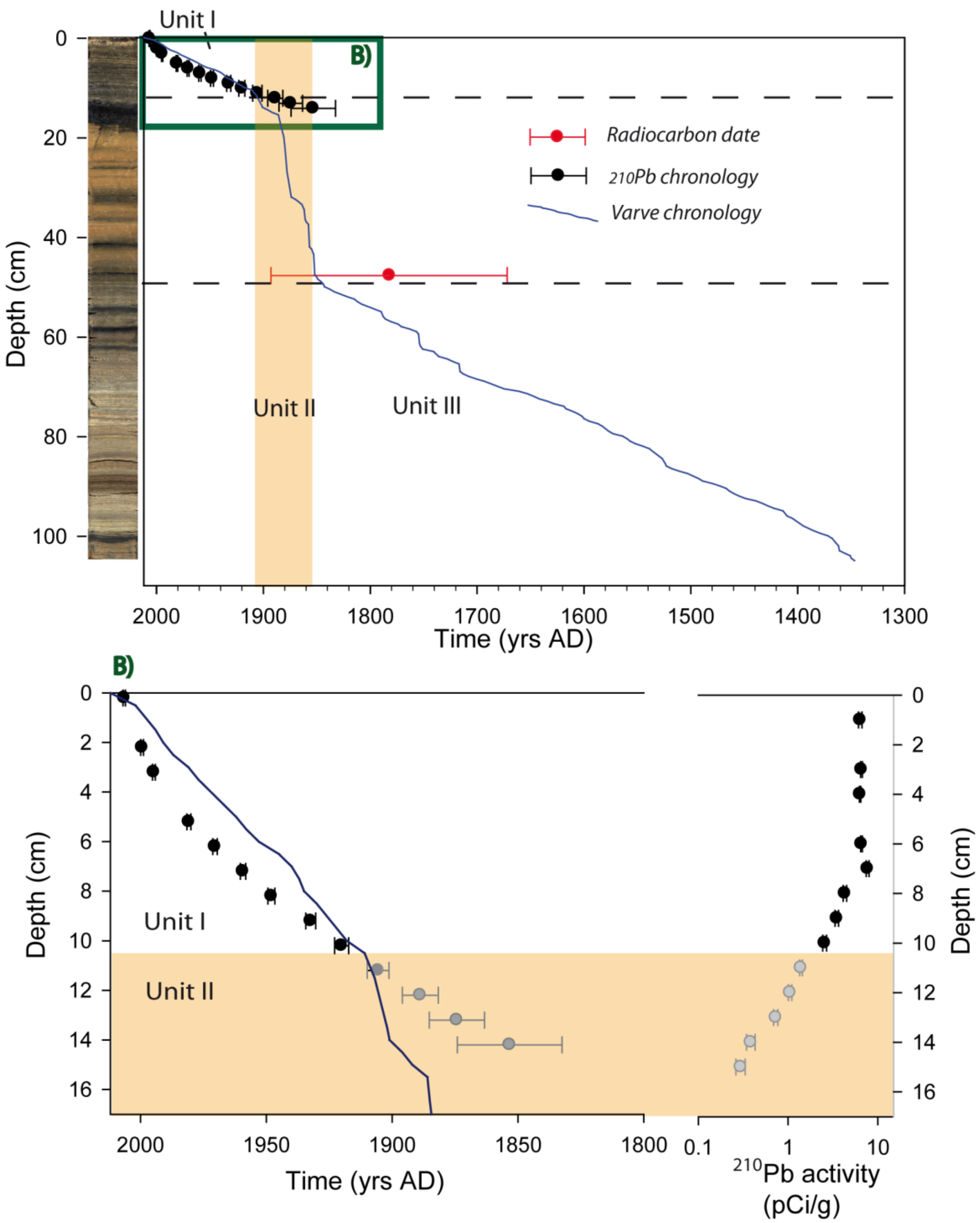
Unit I
B)
Radiocarbon date
210Pb chronology
Varve chronology
Depth (cm)
Unit II
Unit III
Time (yrs AD)
B)
Unit I
Unit II
Depth (cm)
Time (yrs AD)
210Pb activity (pCi/g)

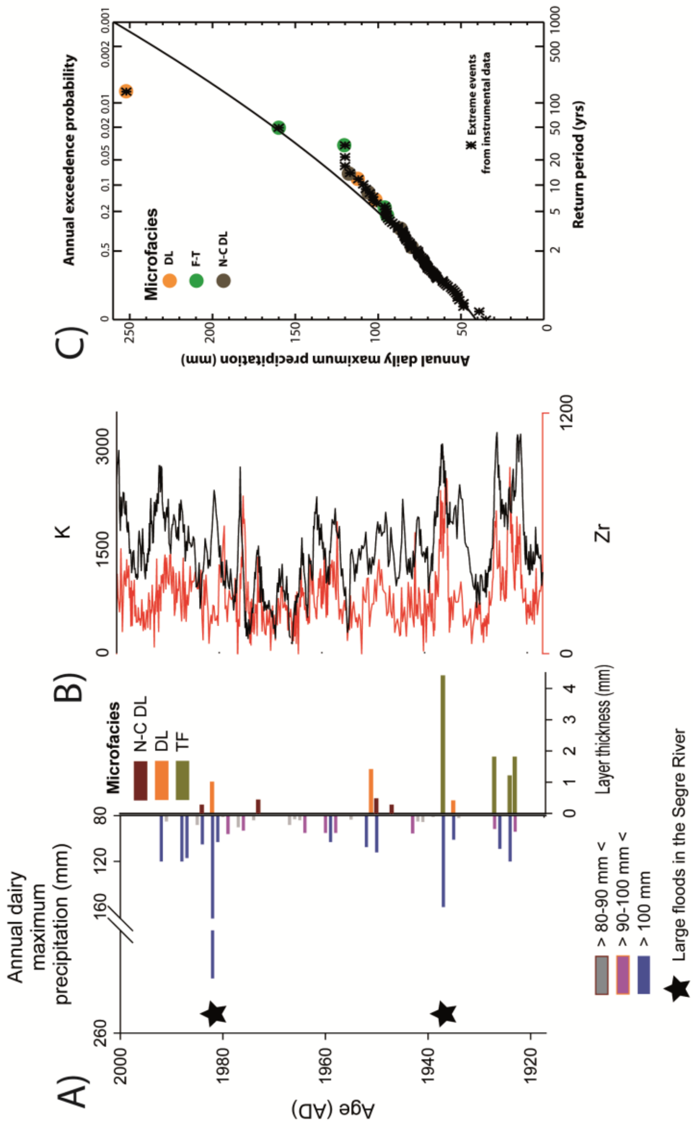
A)
B)
C)
Age (AD)
Annual dairy maximum precipitation (mm)
Microfacies
N-C DL
DL
TF
Layer thickness (mm)
> 80-90 mm <
> 90-100 mm <
> 100 mm
Large floods in the Segre River
K
Zr
Annual exceedence probability
Return period (yrs)
Annual daily maximum precipitation (mm)
F-T
Extreme events from instrumental data

1035

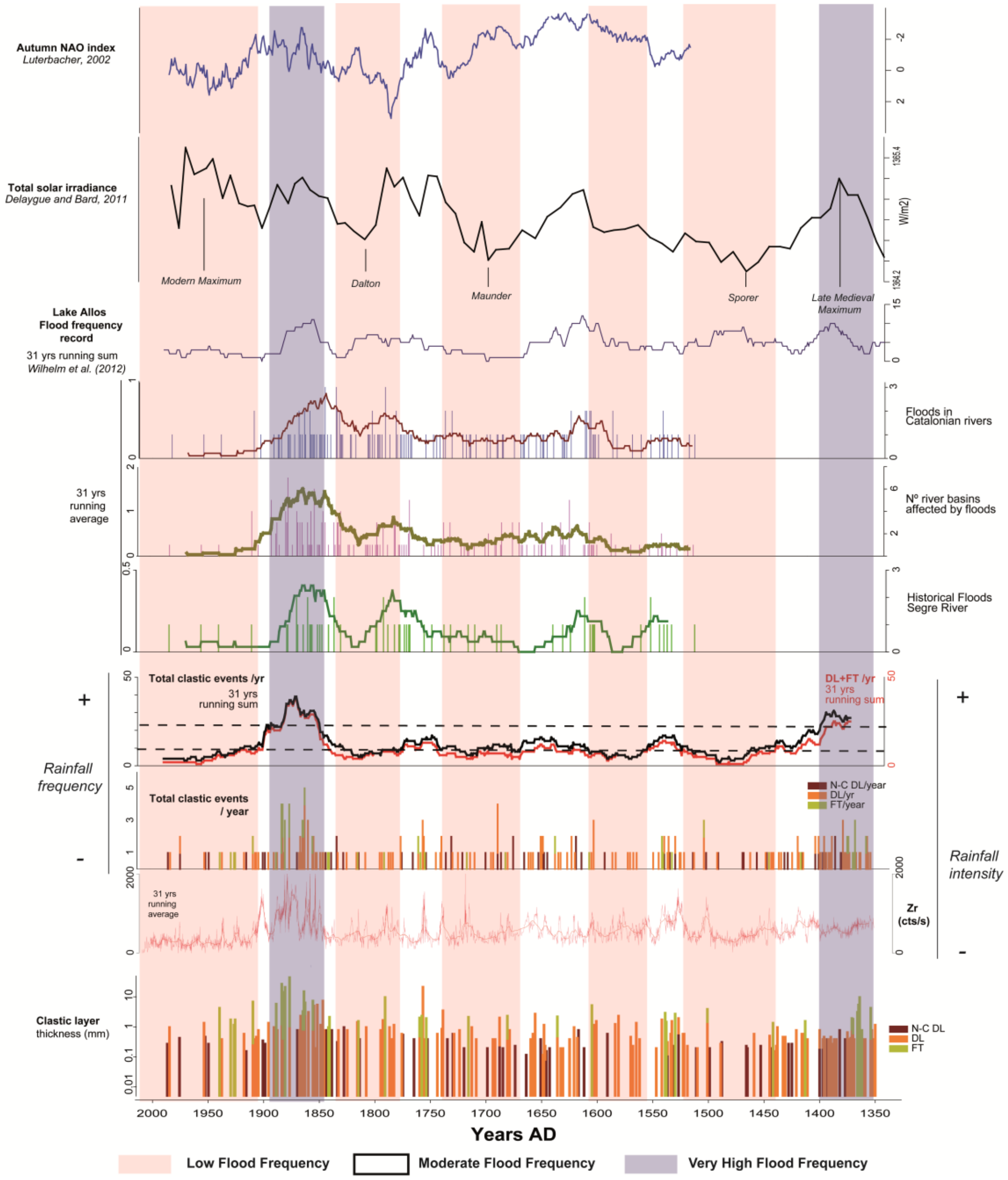

Autumn NAO index
Luterbacher, 2002
Total solar irradiance
Delaygue and Bard, 2011
Modern Maximum
Dalton
Maunder
Sporer
Late Medieval Maximum
W/m2)
Lake Allos
Flood frequency record
31 yrs running sum
Wilhelm et al. (2012)
Floods in Catalonian rivers
31 yrs running average
Nº river basins affected by floods
Historical Floods Segre River
Total clastic events /yr
31 yrs running sum
DL+FT /yr
31 yrs running sum
Rainfall frequency
Total clastic events / year
N-C DL/year
DL/yr
FT/year
Rainfall intensity
31 yrs running average
Zr (cts/s)
Clastic layer thickness (mm)
N-C DL
DL
FT
Years AD
Low Flood Frequency
Moderate Flood Frequency
Very High Flood Frequency